Reshaping Convex Polyhedra: Two Theorems Sketched

Joseph O'Rourke Costin Vîlcu

February 13, 2024

Abstract

In this note we sketch two of the main theorems in the monograph *Reshaping Convex Polyhedra* [OV22a], one from Part I and one from Part II. The proofs, including preliminaries and variations, are about 100 pages each, justifying these sketches.

1 The First Result

Part I of the monograph *Reshaping Convex Polyhedra* [OV22a] contains a proof of this theorem:

Theorem 1 *Every convex polyhedron P can be reshaped to any convex polyhedron $Q \subset P$ via a sequence of $O(n^4)$ digon tailorings.*

Here, n is the maximal number of vertices of P, Q.

We explicate this theorem and sketch its proof. Later (Section 9) we similarly sketch the proof of a theorem from Part II. We largely ignore computational complexities throughout.

With some abuse of notation, we use the term "convex polyhedron" with two meanings. One is for the solid object, e.g. when writing $Q \subset P$. Another one is for the boundary surface, e.g. when considering "digon tailoring". This identification of the two is justified by Alexandrov's Gluing Theorem, introduced in 2.1.

2 Digon Tailoring

A *digon* is a subset of (the surface of) P bounded by two equal-length geodesic segments that share endpoints x and y. A *geodesic segment* is a shortest geodesic between its endpoints. A *digon tailoring* step excises a digon that contains a single vertex v, and then sutures closed the two sides of the digon. Informally, if the surface were made of paper, one could view digon tailoring as pinching a neighborhood of v flat, slicing off v, and then identifying the two sides of the slice. As we will see, the modified surface is again a convex polyhedron.

Fig. 1(a) shows a digon enclosing vertex d, and (b) show the result of excising the digon. In (a,b), the digon endpoints are interior to faces of P. However, either or both could be at vertices. A digon tailoring step always removes one vertex, and either adds two new vertices, or one, or no new vertex. So after suturing, if P has n vertices, the new polyhedron P' has $n+1$, n, or $n-1$ vertices. Although not obvious, P' is a convex polyhedron, in this case of 5-vertices, as

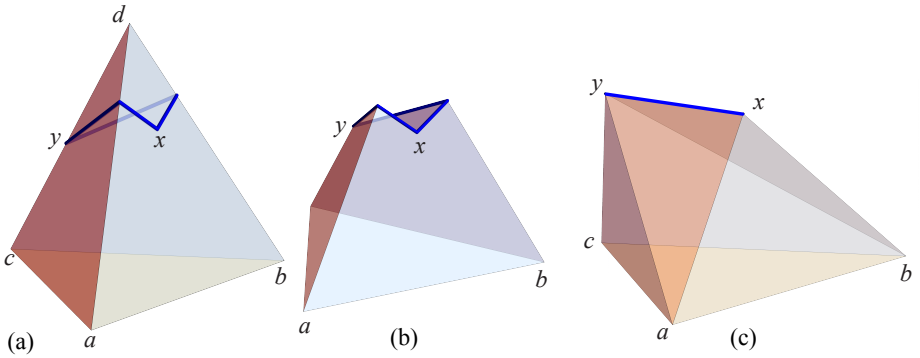

Figure 1: Vertex excision via digon tailoring.

shown in Fig. 1(c).

2.1 Alexandrov's Gluing Theorem

The reason that suturing closed the sides of the removed digon results in a convex polyhedron is Alexandrov's Gluing Theorem [Ale05]:

Theorem [Alexandrov] *Glue together (flexible) planar polygons edge-to-edge such that*

1. *All perimeters are matched: no overlaps, no gaps.*
2. *The glued angle at every point is* $\leq 2\pi$.
3. *The resulting surface is homeomorphic to a sphere.*

Then the resulting surface is isometric to a unique (up to rigid motions and symmetries) convex polyhedron, possibly degenerated to a doubly-covered convex polygon.

As yet there is no effective procedure to construct the three-dimensional shape of the polyhedron guaranteed by this theorem. It has only been established that there is a theoretical pseudopolynomial-time algorithm [KPD09], but this remains impractical in general. Fig. 1(c) was constructed by ad hoc techniques.

Because the sides of the digon are geodesics, gluing them together to seal the hole leaves 2π angle at all but the digon endpoints. The endpoints lose surface

angle with the excision, and so have strictly less than 2π angle surrounding them. So Alexandrov's Theorem applies and yields a new convex polyhedron.

Thus digon tailoring converts a given P to another convex polyhedron P'. Next we describe how to "aim" the tailoring toward a given target $Q \subset P$.

2.2 Slicing

Vertex truncation is analogous to digon tailoring in that it removes a vertex v, but instead by slicing P with a plane and then filling the created hole with new surface forming a convex k-gon face, where k is the degree of v. This is how, for example, the truncated cube can be formed from the cube by 8 vertex truncations.

More generally, we will say a *slicing* of a polyhedron P is removal of a portion of P—perhaps including many vertices—in a half-space bounded by the slicing plane. If $Q \subset P$, it is easy to *sculpt* Q from P by repeatedly slicing P with planes each containing a face of Q. Consider, for example, a tetrahedron Q in the corner of a cube P, as shown in Fig. 2. In this simple case, a single slice

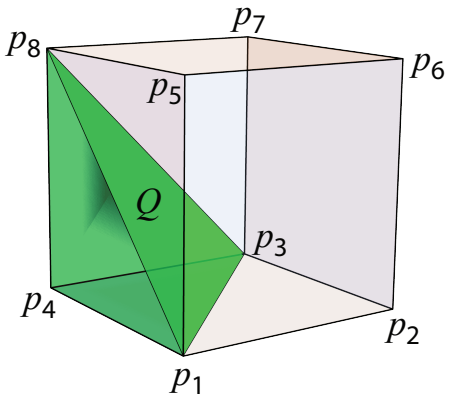

Figure 2: Tetrahedron Q inside cube P.

along the diagonal face $p_1p_3p_8$ sculpts P to Q.

2.3 Algorithm Tracking Sculpting

Our proof of Theorem 1 is constructive, and can be viewed as an algorithm that tracks a sequence of sculpting slices. At the top level, we track a sculpting sequence of slices of P, and for each slice identify a sequence of "stacked" pyramids such that, if each pyramid is reduced to its base by digon tailorings, the pyramids collapse to the slice face of Q.

As ususal, a *pyramid* is the convex hull of a *base* convex polygon X and one point (the *apex*) not on the base plane.

We will illustrate Algorithm 1 with the cube-tetrahedron example (Fig. 2). Fig. 3(a) shows the full cube P.

Algorithm 1: Slices to pyramids.

Input : $Q \subset P$
Output: Stacked pyramids.

for *each face* F *of* Q Π **do**
    `// Conceptually slice` P `with` Π.
    Construct a sequence of stacked pyramids
    whose reductions collapse the pyramids to F.
end
Result: Lists of stacked pyramids.

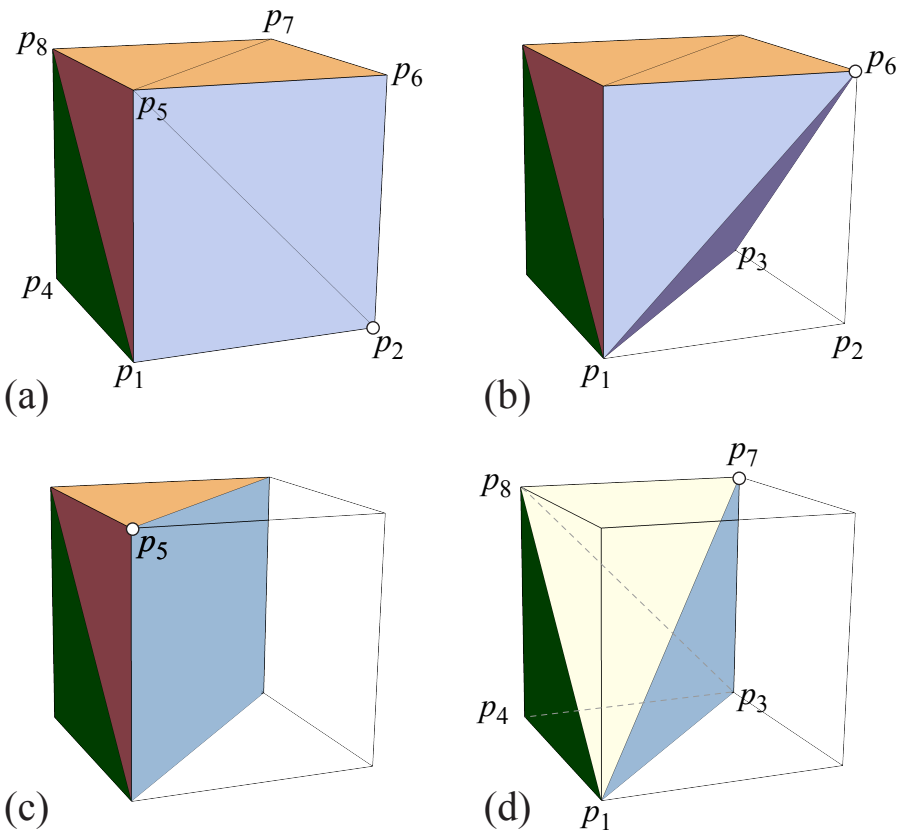

Figure 3: Successive pyramid apexes (marked): p_2, p_6, p_5, p_7.

- The first pyramid collapsed Fig. 3(b) has apex p_2 and base $p_1p_3p_6$.
- The second pyramid to be collapsed Fig. 3(c) has apex p_6 and base $p_1p_3p_7p_5$.
- The third pyramid to be collapsed Fig. 3(d) has apex p_5 and base $p_3p_7p_8$.
- The last pyramid to be collapsed has apex p_7 and base $p_1p_3p_8$.

After that final collapse, the tetrahedron in Fig. 2 has been achieved.

There remain three challenges to turning this high-level algorithm to a proof:

(1) Partition the sliced portion of P into stacked pyramids, achieved in two steps.
   (a) Sliced portion of $P \to$ g-domes (Section 3).
   (b) Each g-dome $\to$ stacked pyramids (Section 4).

(2) Collapsing each pyramid to its base (Section 5).

3 Slice $\to$ Domes

The sense in which the pyramids are "stacked" is that they can be reduced to their bases "outside-in," as in the Fig. 3 example. The way we achieve this is via domes, and in particular, what we call g-domes. A *dome* is a convex polyhedron with every face sharing an edge with its *base* convex polygon X. We generalize this slightly to *g-domes*, with every face sharing an edge or vertex with the base.

Algorithm 2: From one slice Π, $O(n)$ g-domes.

Input : One slice plane Π
Output: $O(n)$ g-domes, a total of at most $O(n)$ vertices.

Let F be the face of Q lying in Π, and e be an edge of F.
Sort vertices angularly about e.
for $i = 0, 1, 2, \ldots, k$ **do**
  Rotate Π_i about e until the portion swept is no longer a g-dome.
  Add to g-domes list.
end
Result: List of $O(n)$ g-domes.

Again we illustrate with the cube-tetrahedron example (Fig. 2). Let $e = p_1p_3$ be the base edge of the slice face $F = p_1p_3p_8$. Rotate a plane Π_i about e, initially Π_0 the entire slice, ending at Π on F, and in between, stopping at every rotation angle whose further rotation would cease to "peel off" a g-dome. In Fig. 4(b), Π_1 partitions off the g-dome whose base is $p_1p_3p_7p_5$ (c), and $\Pi_2 = \Pi$ partitions off the g-dome with base $p_1p_3p_8$ (d). Notice that neither of these pieces is a pyramid. It should also be clear that these g-domes are "stacked" outside-in, by construction.

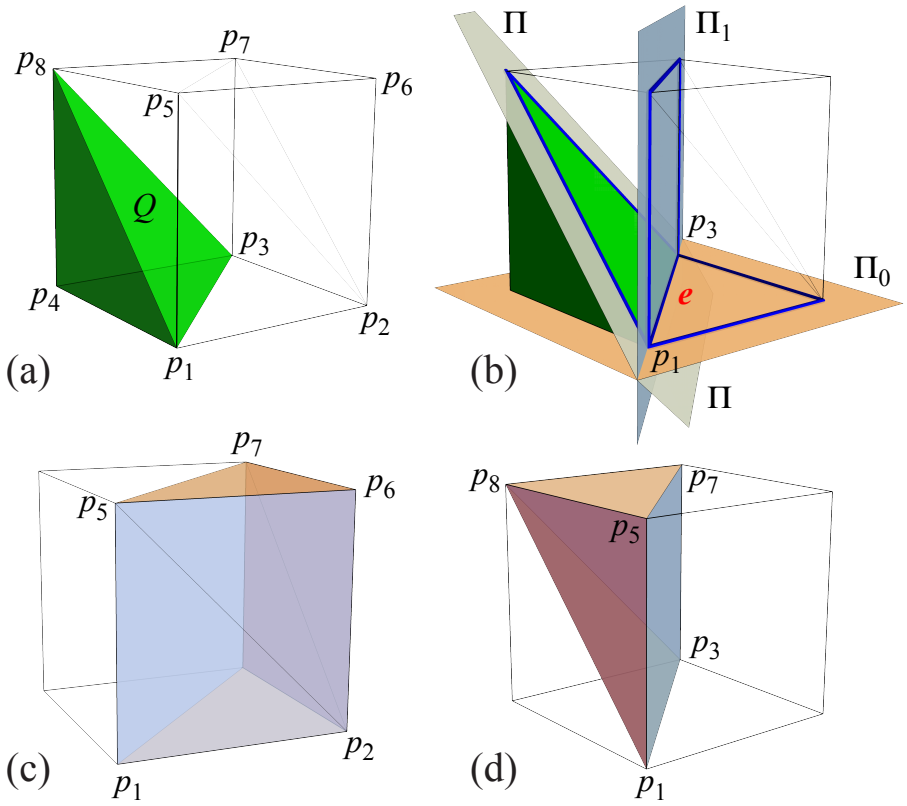

Figure 4: Slice partitioned by rotation (b) into two g-domes (c,d).

4 Domes → Pyramids

Now we come to the two most difficult parts of the proof: Patitioning g-domes to pyramids (exemplified in this section), and reducing pyramids to their bases (Section 5). For the first, we simply claim that methodical slicing of a g-dome reduces it to a series of stacked pyramids. Fig. 5 shows an example g-dome eventually reduced to a pyramid over the same base through a series of pyramid slices that remove all incidences to v_1 one-by-one, leaving v_2 as the apex of a pyramid.

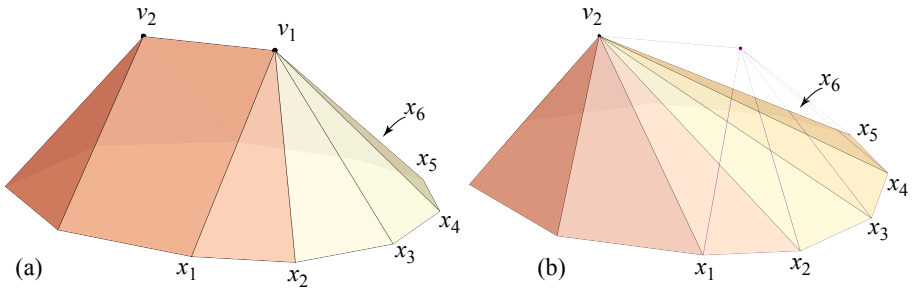

Figure 5: (a) g-dome reduced to (b) pyramid.

5 Pyramids → Base

We have so far not yet invoked digon tailoring. Instead, we have outlined a procedure to track a sculpting of P to $Q \subset P$ to guide partitioning each sculpting slice into a number of g-domes, and each g-dome into a number of pyramids, all stacked with their apexes accessible from the exterior. Finally we come to reducing each pyramid to its base. We illustrate the procedure with

Algorithm 3: Tailor one pyramid P to its base X.

Input : A pyramid P of $O(n)$ vertices, base X.
Output: After removal of $O(n)$ digons, P flattened to X.

`// Assume apex degree-`k`, with` $k = O(n)$.
for *each of* x_i, $i = 1, 2, \ldots, k$ **do**
  Find digon with one endpoint x_i, surrounding y_i.
  Remove digon, suture closed.
  Apply Alexandrov's Gluing Theorem → new convex polyhedron.
end
Result: $O(n)$ digon tailorings flattening P to X.

the pyramid with a regular hexagon base shown in Fig. 6.

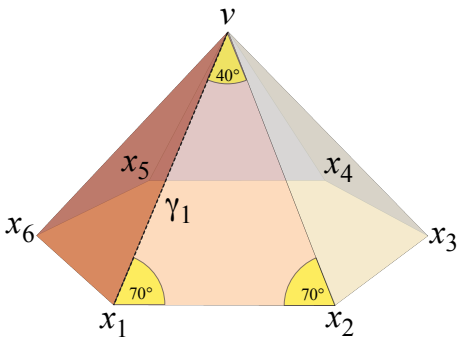

Figure 6: A pyramid with a hexagonal base. Base vertex angle 120° vs. lateral angle 140°.

Starting at base vertex x_1, we locate a digon surrounding the apex $v = y_0$. That digon is excised and its sides sealed; see Fig. 7(a). Continuing counterclockwise, digons are identified with endpoints x_i and y_i. Here we crucially use properties of the cut locus and star-unfolding to ensure that y_i lies on the (images of the) lateral sides of the reducing pyramid instead of lying in the base X. This is one of the most delicate aspects of the proof. The end result is that

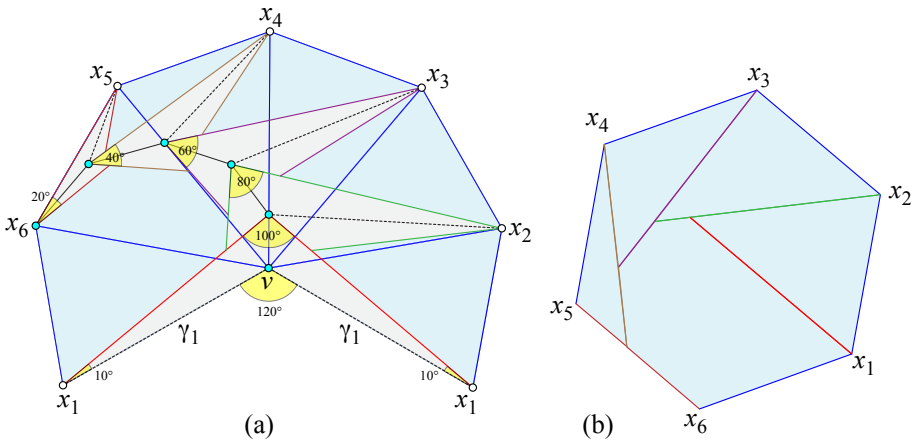

Figure 7: (a) Consecutive digons shaded. Dashed lines are geodesics γ_i from x_i to the point y_{i-1} (with $y_0 = v$). (b) After excising all digons, the pyramid is reduced to its base X. Seals marked.

the pyramid P has been flattened to its base X, with the overlapping digon removals creating *seals* as illustrated in (b).

This completes the sketch of the proof of Theorem 1. Our monograph [OV22a] proves in Part I two similarly universal reshaping theorems.

We should note that although we invoke Alexandrov's Gluing Theorem at several stages of the analysis, we never need the explicit 3D structure of the intermediate polyhedra to construct cut loci, our main tool, which can be calculated via an intrinsic representation of the surface.

6 Enlarging Q to P

Corollary 1 *For any two convex polyhedra P, Q, with $Q \subset P$, Q may be enlarged to P by insertions of surface.*

Proof: (*Sketch*). First tailor P to Q, tracking the cuts and digons removed. Then, starting with Q, cut each sealed geodesic and insert the earlier-removed corresponding digon surface, in reverse order. □

This yields in a sense an "unfolding" Q onto P, extending the usual notion of unfolding a convex polyhedron in the plane.

7 Continuously Folding P onto Q

Corollary 2 *For any two convex polyhedra P, Q, with $Q \subset P$, there exists a continuous non-self-intersecting folding of P onto Q.*

Proof: (*Sketch*). Instead of excising the digon and suturing closed its two sides, gradually bring together the two digon sides, forming a growing doubly-covered triangle, which is folded onto the intermediate surface Q'. Now "meld" the folded triangle into Q''s surface, and repeat. □

Fig. 8 illustrates the main idea. This concept of continuously folding a polyhedron onto another one extends the notion of continuously folding a convex polyhedron onto the plane.

8 An Open Problem

We cite many open problems in [OV22a], but here only repeat one: Corollary 2 establishes existence only. Is there an algorithmic equivalent?

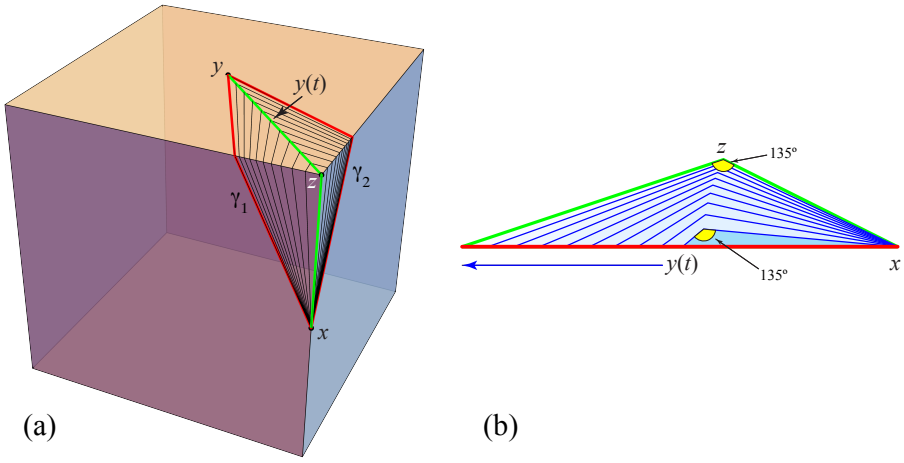

Figure 8: (a) Digon xy surrounding vertex z. $y(t)$ moves along the geosegment zy. (b) Each t leads to a doubly-covered triangle $T(t)$ with apex z and base $xy(t)$. The angle at z is fixed to half of $3\pi/2$ by the curvature of $\pi/2$ at vertex z.

9 The Second Result

Now we describe one of the main theorems from Part II of the monograph *Reshaping Convex Polyhedra* [OV22a] and sketch its proof:

Theorem 2 *Every convex polyhedron P with a simple closed quasigeodesic through at most two vertices, can be embedded on a cylinder as a single connected piece and then rolled to a net on the plane.*

By a *net* we mean unfolding of the surface of P to a simple polygon in the plane. Often this term insists that the edges of the net are edges of P—the unfolding is an edge-unfolding—but here we mean a more *general net* that results from cutting the surface anywhere, an "any-cut" unfolding. We defer defining a quasigeodesic to Section 13.

10 Vertex Merging

In Part I we reduced a polyhedron P by cutting out digon portions of the surface. In Part II we concentrate on what is in a sense the inverse of digon tailoring: insert two congruent triangles of new surface along a geodesic arc, a technique introduced by Alexandrov [Ale05, p. 240]. Let x and y be two vertices of P whose sum of curvatures $\omega(x) + \omega(y)$ is less than 2π, and let γ be a geodesic connecting them. Then one can insert along γ a doubly-covered triangle T with base angles $\frac{1}{2}\omega(x)$ and $\frac{1}{2}\omega(y)$. This has the effect of flattening x and y, and adding one new vertex z, the apex of the triangle T. This is called a *vertex-merge*: x and y are merged into z, which inherits the curvature lost at x and y. The process is illustrated in Fig. 9, which the reader will notice is the reverse process illustrated in Fig. 1. Here γ is an edge of a 5-vertex hexahedron P, although in general it can be any geodesic, as long as x and y satisfy the curvature conditions. After such a vertex-merge, the new surface is a convex

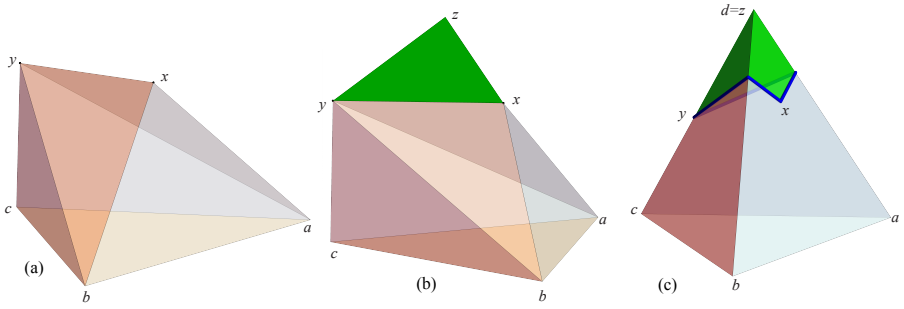

Figure 9: (a,b) Vertex-merge of x and y along $\gamma = xy$ on P. Green indicates surface-inserts. (c) The new polyhedron. (Images not to same scale.)

polyhedron by Alexandrov's Gluing Theorem. Although hardly obvious from (b), the result (c) is a regular tetrahedron.

There are only two classes of *irreducible* polyhedra, i.e., that admit no vertex merge: *isosceles tetrahedra*—those whose vertices all have curvature π—and doubly-covered triangles. Aside from these special cases, one can enlarge any convex polyhedron by repeated vertex-merges until it reaches an irreducible state.

11 Forest of Slits

We called a closed suture resulting from digon tailoring a *seal*; we now call the geodesic γ supporting a vertex-merge a *slit*. As our goal in Theorem 2 is to result in a single-piece net, we want the *slit graph* to be a forest of trees. For any cycle in the slit graph will separate the surface into disconnected pieces.

We now describe in some detail how Theorem 2 applied to the cube in Fig. 10 leads to a net. We perform all together six vertex-merges, three on the top face vertices and symmetrically three on the bottom face vertices. In (a) of the figure, we first merge v_7 and v_8 by inserting a doubled right triangle (yellow) along the slit edge v_7v_8. The $\frac{\pi}{2}$ surface added to v_7 and v_8 flattens both vertices, and they are replaced by v_{78}.

Next we merge v_5 with v_{78} along the indicated geodesic, flattening both of those and creating a vertex v_{578} at the tip of the inserted doubly-covered triangle (blue).

The angle incident to the merge vertex v_{578} is $\frac{\pi}{2}$, and the angle incident to the as-yet unmerged top vertex v_6 is $\frac{3\pi}{2}$. So technically we cannot merge v_{578} with v_6 because the curvatures sum to 2π. However, we can imagine a merge resulting in a pair of parallelograms (rather than triangles). If we cut the surface along the geodesic segment v_6v_{578} (of length $2\sqrt{2}$ for a unit cube) and insert the parallelograms, the result is a cylinder as depicted in Fig. 10(b). Note the two $\frac{\pi}{4}$ angles inserted at v_6 flatten that vertex, and the insertion of the two $\frac{3\pi}{4}$ angles flattens v_{578}.

Finally, symmetric merges on the bottom-face vertices leads to embedding the cut cube onto an unbounded cylinder in both directions.

Note that the three slits on the top face of the cube form a tree, as do the slits on the bottom face. Thus we have reduced the cube to a cylinder by slits forming a forest of—in this case two—trees. So we have not disconnected the original cube surface. And therefore rolling the cylinder on the plane unfolds the cube to a non-overlapping net: see Fig. 11.

12 Spiral Slit Tree: the 2D model

The three vertex-merges on the top of the cube in Fig. 10(a), and the three on the bottom, are what we call *sequential merges*: at each step, the newly created merge vertex is connected to an as-yet unmerged vertex: v_{78} to v_5, and v_{578} to v_6. In particular, we choose a *spiral* merge order, which we illustrate in 2D in Fig. 12. Here a slit is a line segment s, and each triangle insert degenerates

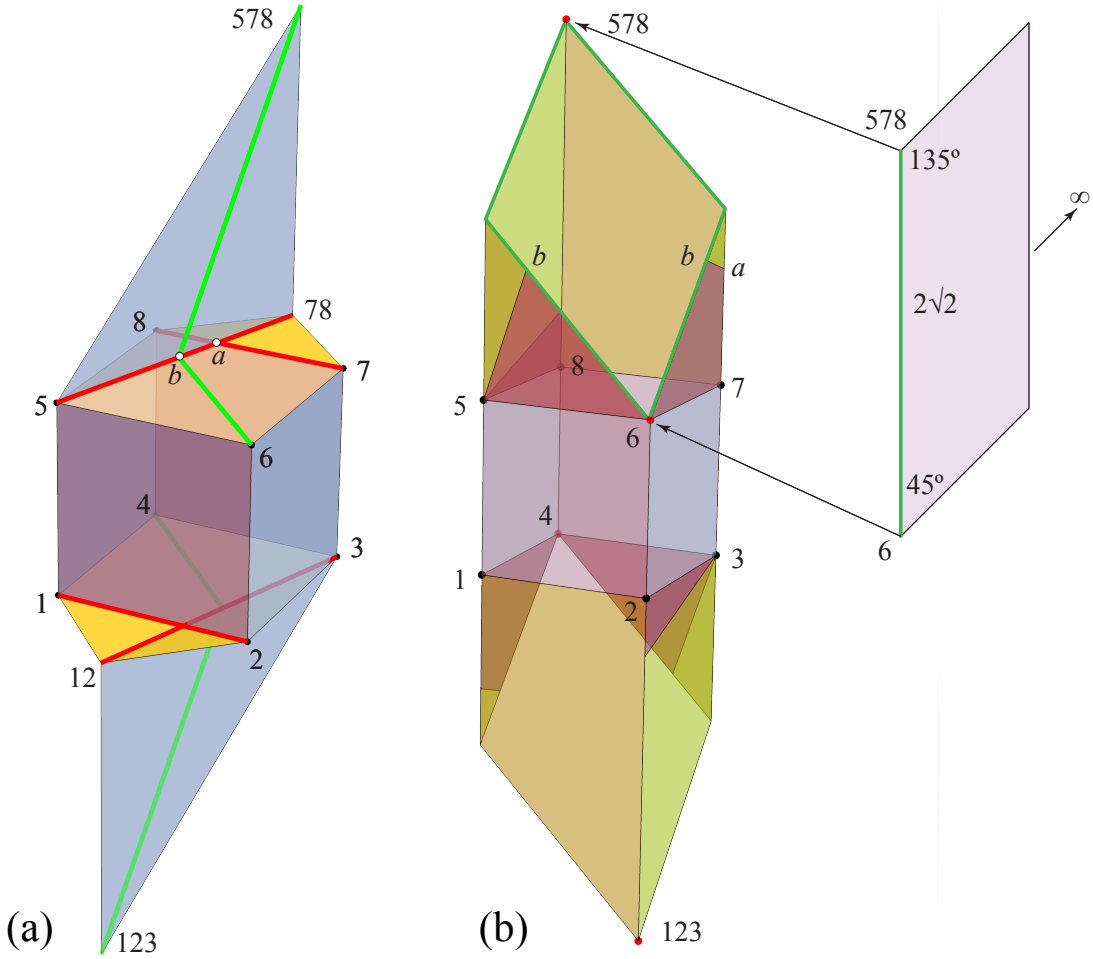

Figure 10: (a) Cutting along the v_6v_{578} geodesic segment (green), and inserting double parallelograms (b) leads to a cylinder. In (b) the yellow regions are inserted merge triangles; pink regions pieces of the top and bottom cube faces.

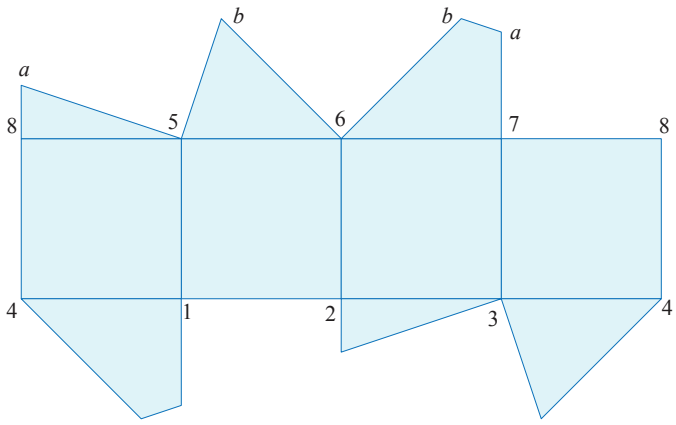

Figure 11: Unfolding of cube to a net by rolling the cylinder on the plane. Labels correspond to those in Fig. 10.

to just s, and creates a merge vertex somewhere along s. First two vertices on the convex hull of the vertex set V are merged, and from then onward, the merges occur in a counterclockwise order on reduced nested hulls of the remaining vertices. We proved that, following this ordering, the slit graph Λ is a tree.

13 Quasigeodesics

The cube has a simple closed geodesic between and paralleling the top and bottom face rims, which naturally partitions the vertices into two sets. To mimic the 2D spiral construction on P in $\mathbb{R}^3$, we need a similar partition. Most convex polyhedra have no simple closed geodesic, but every one has a simple closed *quasigeodesic*. A quasigeodesic has at most π surface angle on either side, and so can pass through vertices. By a theorem of Pogorelov [Pog49], every convex polyhedron has at least three simple closed quasigeodesics. An example of a 2-vertex quasigeodesic on a regular tetrahedron is shown in Fig. 13.

Recently an exponential algorithm was developed to find one such quasigeodesic [CdM22]. Henceforth, we will assume that Q is a simple closed quasigeodesic on P, partitioning P into two "halves" P^+ and P^-.[1]

14 Convex Hull on Half Surface

As is evident from the 2D spiral merge model in Fig. 12, to extend that process to 3D requires taking the convex hull of a set of vertices on P. Although there are

[1]Note the symbol Q in Part II represents a quasigeodesic, not a polyhedron as it did in Part I.

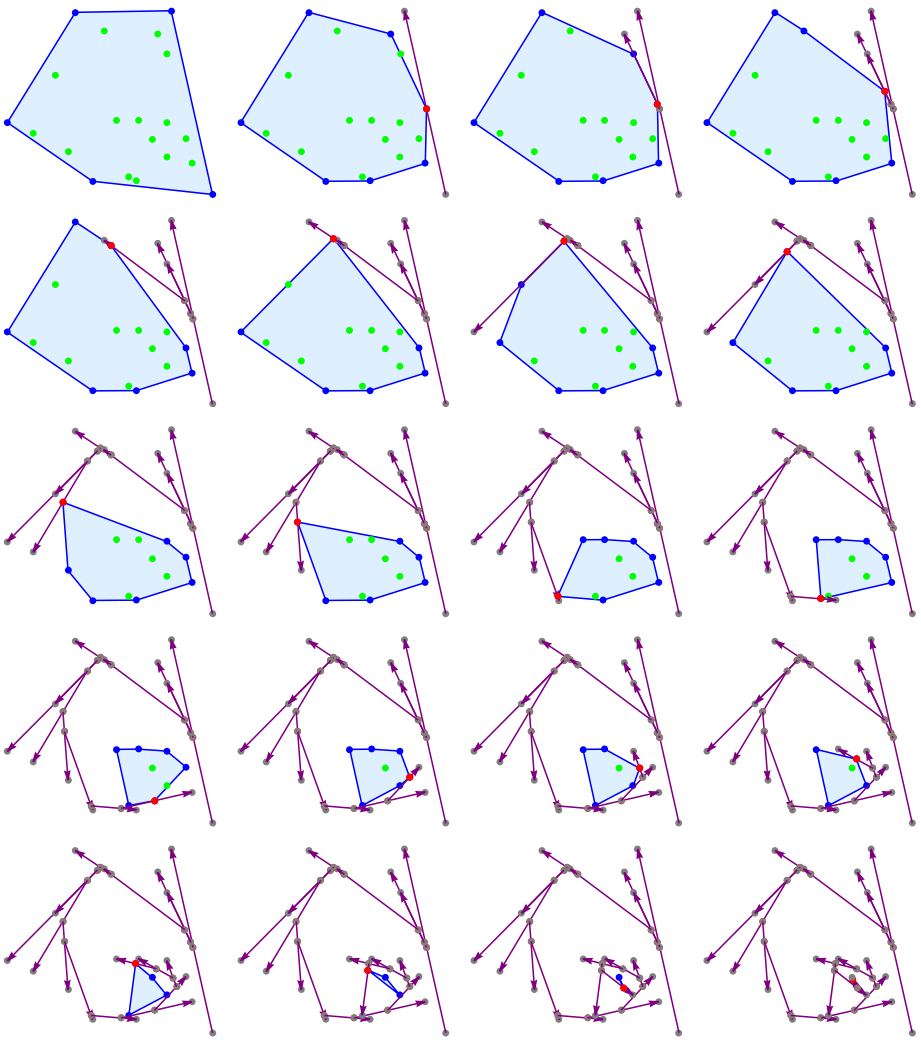

Figure 12: Trace of 2D spiral merges with $|V| = 20$.

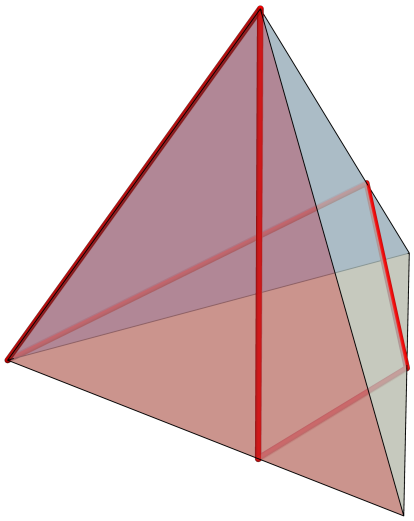

Figure 13: A 2-vertex simple closed quasigeodesic. From [OV22b].

several definitions of convexity on P in the literature, none satisfy our needs. To cite just one example, applying the definition of the "metric-convex hull" in [GM01] to the set of vertices of P does not result in the entire surface of P as the hull, which we find unnatural. In contrast, if we define a set S as *convex* if every geodesic segment between two points of S is in S, and the *convex hull* of S as the smallest convex set enclosing S, then the hull of the vertices of P is the whole of P.

Still, there remains a serious problem for our application: If S is a set of vertices V, two of which are vertex-merged, the hull of the new set V' can enclose S, counter to intuition and counter to our needs. This leads us finally to define the *relative convex hull*, $\mathrm{rconv}(V)$, of a set of vertices V in either P^+ or P^-. This resolves the issue with vertex-merging: the new hull after a merge just adds the inserted triangles to the interior of the hull. Moreover, $\mathrm{rconv}(V)$ for $V \subset P^+$ can be constructed in polynomial time.

A second—and different—notion of convex hull, based on the minimal length enclosing polygon, is also developed in [OV22a], with similar unfolding consequences.

15 Spiral Slit Tree in 3D

One of the more intricate components of the proof of Theorem 2 is proving the properties of the spiral vertex-merging on P^+. We only sketch the process, referencing Fig. 14. Here V is the six vertices on the half-surface P^+ of a regular icosahedron, above a simple closed geodesic Q (not shown). $\mathrm{rconv}(V)$ is the pentagon $v_1v_2v_3v_4v_5$ enclosing v_6.

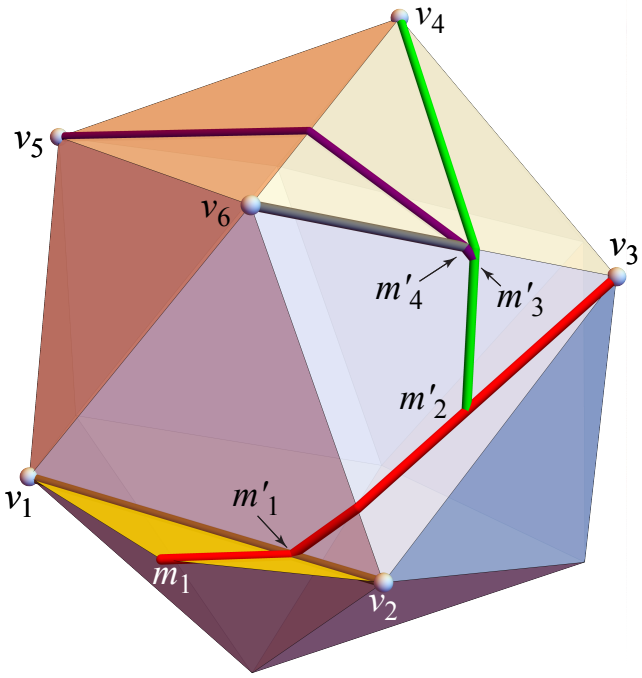

Figure 14: The vertex-merge cuts on a regular icosahedron P.

First v_1 is merged with v_2, and a doubly-covered triangle (yellow) is inserted along v_1v_2, with apex m_1. At this stage, Alexandrov's Gluing Theorem is applied to produce a new polyhedron P', and $\mathrm{rconv}(V') = m_1v_3v_4v_5$. Next, m_1 is merged with v_3, and a (large) doubly-covered triangle is inserted along the geodesic segment m_1v_3 (red). The apex m_2 is not shown, but instead the point m'_2 is where the next geodesic segment m_2v_4 (green) enters P on its way to v_4. Continuing in this manner, all six vertices are merged, the last one, m_4 to v_6 (gray) resulting in a cylinder analogously to the situation with the cube in Fig. 10(b). Because the slit graph Λ is a tree, we have not disconnected the original P. See Fig. 15.

Repeating the merging on P^-, and joining the two symmetric half-cylinders together, permits rolling on the plane to produce a net for the icosahedron. This accords with the claim of Theorem 2.

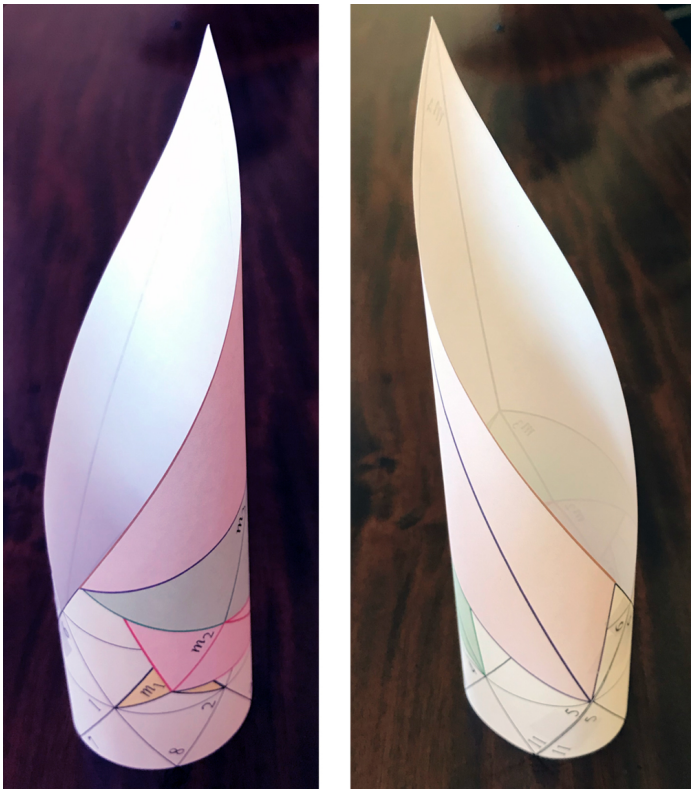

Figure 15: The half-cylinder obtained from Fig. 14.

16 The Quasigeodesic Condition

The reason Theorem 2 requires that the quasigeodesic Q includes at most two vertices is somewhat subtle. The two examples we detailed both have natural Q through zero vertices—geodesics, so the issue did not arise.

Suppose Q contains vertices q_1 and q_2. Then applying the spiral merge on P^+ will first merge q_1, q_2 along the slit γ_{12}, producing a merge vertex $m^+ \in P^+$. Similarly, the spiral merge on P^- will include γ_{12} and produce $m^- \in P^-$. The γ_{12} slit connects the two slit trees Λ^+ and Λ^-.

But now if Q contains a third vertex q_3, then m^+ will merge with q_3 along a slit in P^+, as will m^- along a slit in P^-. These merges create slits that form a cycle connecting γ_{12} to q_3 in both P^+ and P^-, disconnecting P.

Without the ≤ 2 condition on Q, we can only prove that P can be embedded on the union of two cones, one for each of P^+, P^-. It still may be possible to roll one cone and then the other to obtain a net for P, but we have only established that under certain conditions.

17 Another Open Problem

The previous remarks lead to this problem: Prove or disprove that every convex polyhedron has a simple closed quasigeodesic through at most two vertices. We have only proved this in a few special cases, e.g., doubly-covered convex polygons [OV22a], and tetrahedra [OV22b].

References

[Ale05] Aleksandr D. Alexandrov. *Convex Polyhedra*. Springer-Verlag, Berlin, 2005. Monographs in Mathematics. Translation of the 1950 Russian edition by N. S. Dairbekov, S. S. Kutateladze, and A. B. Sossinsky.

[CdM22] Jean Chartier and Arnaud de Mesmay. Finding weakly simple closed quasigeodesics on polyhedral spheres. In *38th Symp. Comput. Geom. (SoCG)*, Leibniz Internat. Proc. Informatics (LIPIcs), pages 27:1–27:16, June 2022. `https://arxiv.org/abs/2203.05853`.

[GM01] Clara I. Grima and Alberto Márquez. *Computational Geometry on Surfaces*. Kluwer Academic, Dordrecht, 2001.

[KPD09] Daniel Kane, Gregory N. Price, and Erik D. Demaine. A pseudopolynomial algorithm for Alexandrov's theorem. In *Workshop Algorithms Data Struct.*, pages 435–446. Springer, 2009.

[OV22a] Joseph O'Rourke and Costin Vîlcu. Reshaping convex polyhedra. arXiv 2107.03153v2 [math.MG]: `arxiv.org/abs/2107.03153`, May 2022.

[OV22b] Joseph O'Rourke and Costin Vîlcu. Simple closed quasigeodesics on tetrahedra. *Information*, 13:238–258, May 2022.

[Pog49] Aleksei V. Pogorelov. Quasi-geodesic lines on a convex surface. *Mat. Sb.*, 25(62):275–306, 1949. English transl., *Amer. Math. Soc. Transl.* 74, 1952.